Communication

Journal of Photopolymer Science and Technology
Volume 30, Number 1 (2017) 99 – 102 ©2017SPST

Photoreactions of Tin Oxo Cages, Model EUV Photoresists

Jarich Haitjema[1], Yu Zhang[1], Niklas Ottosson[1], and Albert M. Brouwer [1,2*]

[1] Advanced Research Center for Nanolithography,
P.O. Box 93019, 1090 BA Amsterdam, The Netherlands
[2] van 't Hoff Institute for Molecular Sciences, University of Amsterdam,
P.O. Box 94157, 1090 GD Amsterdam, The Netherlands
**f.brouwer@arcnl.nl*

Organotin oxo cage compounds have an electronic absorption band in the UV spectral range (λ_{max} ~220 nm) associated with a σd electronic transition. Irradiation at 225 nm of thin films of these materials leads to loss of carbon, as shown by X-ray Photoelectron Spectroscopy. Photolysis of solutions of the compounds causes a decrease and slight broadening of the absorption band, consistent with replacement of the organic groups. Quantum chemical calculations support the breaking of the tin-carbon bonds as the primary process, both in electronically excited states and in oxidized states that can be expected to be the result of EUV photoionization.

Keywords: Metal-organic, Photoresist, Photoreaction, Quantum chemistry

1. Introduction

For Extreme Ultraviolet (EUV) Lithography (EUVL) to firmly grasp its position as a tool for mass production of nano-electronic devices, the availability of suitable photoresists is an important condition [1,2]. Photoresists based on acid-catalyzed polymer deprotection, which are the standard for deep UV photolithography, have in the past decade been adapted for use in EUVL [3]. These materials have a number of inherent limitations related to diffusion of the catalyst and to the stochastic distributions of photoacid generators (PAG) and quenchers. Probably even more importantly, the absorption cross-sections of these mostly organic materials at the EUV wavelength of 13.5 nm are only low, [4,5] and their resistance to etch processes is limited. These disadvantages are aggravated by the need to reduce the film thickness in order to maintain a reasonable aspect ratio for the small features that need to be transferred. As an approach to overcome these limitations, metal-containing materials have been proposed by a number of research groups [6-8].

In this work, we study the class of tin cage compounds that was introduced to the EUV lithography field by Brainard and co-workers [7]

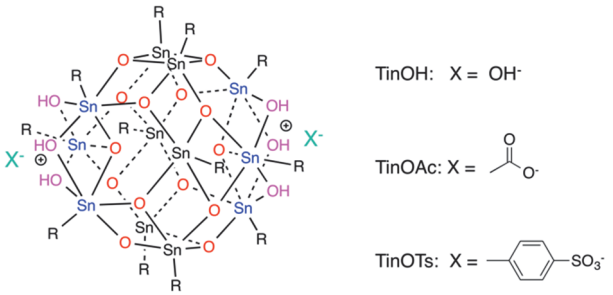

Scheme 1. Molecular structures of the tin cage compounds studied. R = n-butyl.

(Scheme 1).

These systems combine several advantages: the demonstrated EUV patterning underscores their relevance for the EUVL field [7,9], the absorption cross sections are 2 – 3 times higher than those of organic polymers [5], and the materials are of a molecular nature, consisting of small (~1 nm) and fully defined building blocks. The goal of our research in this field is to boost the fundamental level of understanding of the photoresist performance in relation to the chemical processes that take place upon activation of these materials by high energy sources such as UV and EUV photons as well as electrons. Apart from the publication by

Received April 25, 2017
Accepted May 12, 2017

the Brainard group [7], and a description of this type of molecular structure as EUV photoresists in an Inpria patent [10], we could not find any publications on the chemical reactivity of this type of tin cage compounds. Their only application sofar seems to be as a filler in polymers, in which their mechanical properties are exploited [11,12].

In the present paper, we focus on the response of **TinOAc** (Scheme 1) to deep UV irradiation. UV photon absorption leads to the formation of a well-defined electronically excited state. Whether such states are also involved in the radiation chemistry induced by EUV excitation is still a matter of debate [13]. In any case, they are relevant in view of the presence of out-of-band radiation in EUVL scanners [14].

2. Experimental and computational methods

Preparation of the compounds, largely following the literature [15,16] and of thin films of **TinOAc** has been described recently [9]. The thickness of the films was 30 nm, as determined by means of AFM and ellipsometry.

The deep UV irradiation was performed using an ESKPLA NT342B laser, delivering 225 nm pulses at 10 Hz with an energy of ~2.5 mJ/pulse. UV-vis spectra were recorded on a Shimadzu UV-2700.

Quantum-chemical calculations were performed using the Gaussian09 program (rev. D1) on a model system **1** in which the n-butyl groups were replaced by methyl groups. Because of the large size of the molecules and the difficulty of geometry optimization of the flexible methyl rotors we were limited [17] to the relatively small LANL2DZ basis set. The standard B3LYP and ωB97DX density functionals were used.

3. Results and discussion

3.1. Molecular structure

The DFT calculations of **1** give rise to optimized molecular geometries in good agreement with available crystal structure data [18-20] (Fig. 1). The tin cage has two different types of tin atoms. In a central belt formed by six four membered Sn-O-Sn-O rings connected via the Sn atoms, each Sn atom is linked to four oxygen atoms and one carbon. The cage is closed on both sides of the central belt by a cap in which three Sn atoms are bridged by OH groups, linked to the central belt, and linked to each other by an oxygen atom inside the cage. These Sn atoms have five bonds to oxygen and one to carbon. The highest occupied and lowest unoccupied molecular orbitals are shown in Fig. 2.

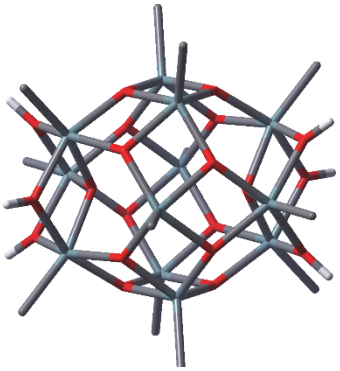

Fig. 1. Computed structure of the tin cage model compound **1** (B3LYP/LANL2DZ). Hydrogen atoms on carbon omitted for clarity.

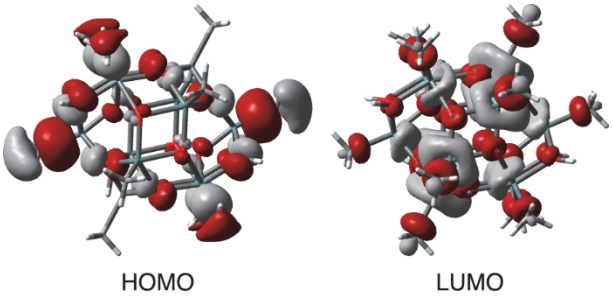

Fig. 2. Highest occupied (HOMO) and lowest unoccupied (LUMO) molecular orbitals of the tin cage model **1** (B3LYP/LANL2DZ).

The highest occupied MO's are located primarily on the Sn-C bonds of the six-coordinated Sn atoms on the caps and may be described as σ-MOs. The LUMO is located on the central belt and is composed mostly of d-orbitals on Sn atoms. Evidently, any chemical process that removes electron density from the HOMO will weaken the Sn-C bonds. In fact, at the current level of theory, geometry optimization after one-electron oxidation or formation of the triplet excited state leads to spontaneous cleavage of an Sn-C bond. This reaction occurs specifically at the sites of the 6-coordinated Sn, where the highest occupied MOs are located.

3.2. Photochemical conversion in solution

The tin cage compounds were found to have a strong absorption near 220 nm, with a decadic molar absorption coefficient $\varepsilon \approx 10^5$ L mol^{-1} cm^{-1}. The conversion of a solution of **TinOAc** in ethanol upon irradiation at 225 nm was monitored using UV/Vis absorption spectroscopy (Fig. 3).

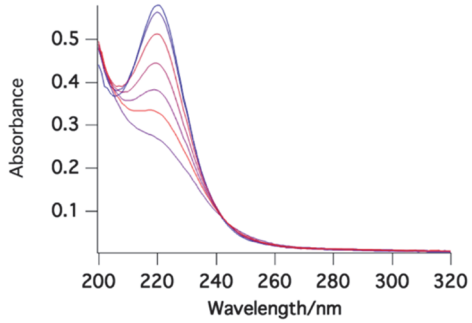

Fig. 3. UV/Vis absorption spectra of a solution of **TinOAc** in ethanol during irradiation at 225 nm. The absorbance at the maximum decreases with increasing time of irradiation.

The experimental absorption spectra show a decrease of the absorption at the maximum of the band, and a slight broadening at the long wavelength edge as the photochemical conversion proceeds. While we are still in the process of a full chemical analysis of the reaction products, we can propose a hypothetical explanation of the observations. Inspired by the DFT calculations we assume that the butyl groups are split off in the primary excited-state process. The tin-centered radicals formed in this way might abstract a hydrogen atom from the butyl radical, from another butyl side chain, or from the solvent ethanol, which is a good hydrogen atom donor. Replacement of the alkyl group by an oxygen substituent is another possible mode of reaction. We modeled this using OH-groups. Interestingly, after replacing one alkyl group (methyl in the model compound **1**) by OH or H, excitation to the triplet excited state leads again to a spontaneous loss of an alkyl group, and this can be repeated until all six methyl groups have been replaced. For each structure, time-dependent density functional theory (TDDFT) was used to compute the UV absorption spectrum. During the evolution of the structures in which the methyl groups are gradually replaced the calculated spectra become broader and less intense as more transitions become allowed and the transition probability is shared among more transitions (Fig. 4). For the OH-substitutions, a red shift is predicted. The TDDFT calculations predict excitation energies slightly higher than what is experimentally observed, but this is in line with common experience. When comparing the two sets of calculations (Fig. 4) with the experimental data in Fig. 3, it appears more likely that the Sn atoms upon irradiation are reduced to hydrides rather than oxidized.

While more chemical analytical work is needed to test its correctness, the current hypothesis at least explains the spectral evolution during the irradiation.

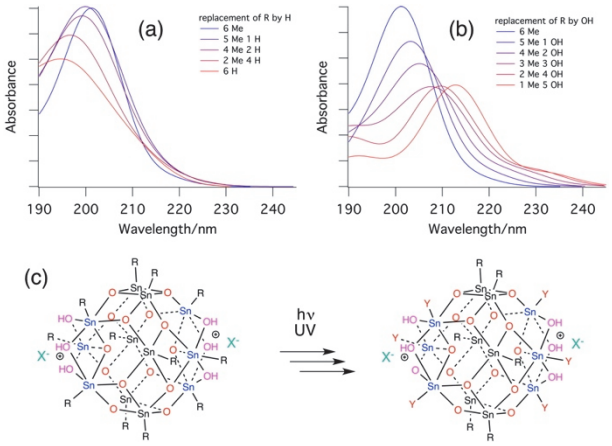

Fig. 4. Computed UV/Vis absorption spectra (TDDFT B3LYP/LANL2DZ) of **1**, and a series of compounds in which the methyl groups at the 6-coordinated Sn atoms are successively substituted. (a) Me replaced by H-atoms (b) Me replaced by OH-groups. (c) Illustration of the stepwise replacement of the alkyl groups of **1** (Y = H or OH).

3.3. Photochemistry in the solid state

Spin-coated films of **TinOAc** were exposed to the same 225 nm laser light as the solutions, and analyzed using Hard X-ray Photoelectron Spectroscopy (HAXPES) [21]. Samples were exposed either under ambient conditions, or in a special sample cell in nitrogen atmosphere. The latter samples were carefully stored under nitrogen until they could be transferred to the HAXPES sample chamber. The spectrum (Fig. 5) of the fresh sample shows the signals of the elements present in the ratios Sn : C : O = 12 : 51 : 25, very close to those expected for the chemical composition $C_{52}O_{24}Sn_{12}$.

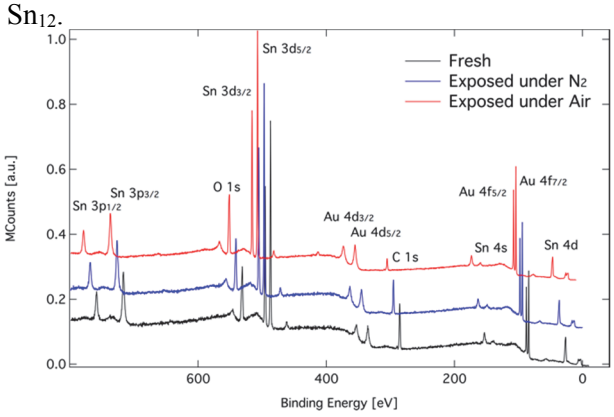

Fig. 5. HAXPES spectra of thin films of **TinOAc**: fresh sample, sample exposed to DUV (1.2 J cm^{-2}) under N_2 and sample exposed to DUV under air. The spectra are scaled to equal intensities of the Sn 3d peaks. The spectra of the exposed samples are offset and shifted for clarity.

After DUV exposure a dramatic loss of carbon relative to Sn is observed. In nitrogen atmosphere,

oxidation cannot occur (Sn : C : O = 12 : 38 : 24), but in the case of the ambient conditions a clear increase in the oxygen content was observed and more carbon was lost (Sn : C : O = 12 : 16 : 30).

The observations are similar to those published recently for **TinOH** [21]. Further analysis of the spectra will be presented elsewhere.

3.4. Common elements of deep UV and EUV induced chemistry

EUV photons have much higher energy than DUV photons, and can be expected to lead to ionization as a primary process. Subsequently, Auger electron emission is likely to fill the core hole formed, leading to a doubly ionized system. Secondary electrons may have enough energy to create other singly and even doubly ionized cages. Interestingly, the DFT calculations on the triplet state, the trication and the tetracation indicate that the same initial process takes place in all cases: barrierless cleavage of the tin-carbon bonds. The details of the subsequent processes, including the quantitative aspects, are the targets of our current research.

4. Conclusion

Butyl-tin cage compound **TinOAc** responds to deep UV irradiation by breaking of the tin-carbon bonds. When thin films are irradiated under ambient conditions, oxygen containing products are formed, but in a solution in ethanol the main products are different, possibly tin hydrides. This work is a step towards knowing and understanding the radiation induced processes in tin oxo cage compounds, which are prototypical EUV photoresists. More complete analysis of the products and quantification of the reaction efficiencies are in progress.

Acknowledgements

This work has been carried out at the Advanced Research Center for Nanolithography (ARCNL), a public-private partnership of the University of Amsterdam (UvA), VU University Amsterdam (VU), the Netherlands Organisation for Scientific Research (NWO) and the semiconductor equipment manufacturer ASML. We thank Michiel Hilbers for help with the irradiation experiments, Andreas Lindblad for help with the HAXPES experiments and Sonia Castellanos for helpful discussions.

References

1. A. Lio, *Proc. SPIE*, **9776** (2016) 97760V.
2. J. W. Thackeray, *J. Micro/Nanolith. MEMS MOEMS,* **10** (2011) 033009.
3. H. Nakagawa, T. Naruoka, and T. Nagai, *J. Photopolym. Sci. Technol.,* **27** (2014) 739.
4. R. Fallica, R. Kirchner, Y. Ekinci, and D. Mailly, *J. Vac. Sci. Technol. B,* **34** (2016) 06K702.
5. R. Fallica, J. Haitjema, L. Wu, S. Castellanos, A. M. Brouwer, and Y. Ekinci, *Proc. SPIE,* **10143** (2017) 101430A.
6. J. Stowers and D. A. Keszler, *Microelectron. Eng.,* **86** (2009) 730.
7. B. Cardineau, R. Del Re, M. Marnell, H. Al-Mashat, M. Vockenhuber, Y. Ekinci, C. Sarma, D. A. Freedman, and R. L. Brainard, *Microelectron. Eng.*, **127** (2014) 44.
8. M. Toriumi, Y. Sato, R. Kumai, Y. Yamashita, K. Tsukiyama, and T. Itani, *Proc. SPIE,* **9779** (2016) 97790G.
9. J. Haitjema, Y. Zhang, M. Vockenhuber, D. Kazazis, Y. Ekinci, and A. M. Brouwer, *Proc. SPIE,* **10143** (2017) 1014325.
10. S. T. Meyers, J. T. Anderson, J. B. Edson, K. Jiang, D. A. Keszler, M. K. Kocsis, A. J. Telecky, and B. Cardineau, US patent 20160116839A1, (2016).
11. F. Ribot, F. Banse, C. Sanchez, M. Lahcini, and B. Jousseaume, *J. Sol-Gel Sci. Technol.,* **8** (1997) 529.
12. W.-Q. Fan, J. Feng, S.-Y. Song, Y.-Q. Lei, G.-L. Zheng, and H.-J. Zhang, *Chem. Eur. J.,* **16** (2010) 1903.
13. A. Narasimhan, S. Grzeskowiak, J. Ostrander, J. Schad, E. Rebeyev, M. Neisser, L. E. Ocola, G. Denbeaux, and R. L. Brainard, *Proc. SPIE,* **9779** (2016) 97790F.
14. T. Itani and T. Kozawa, *Jpn. J. Appl. Phys.,* **52** (2013) 010002.
15. C. Eychenne-Baron, F. Ribot, and C. Sanchez, *J. Organomet. Chem.,* **567** (1998) 137.
16. L. Van Lokeren, R. Willem, D. van der Beek, P. Davidson, G. A. Morris, and F. Ribot, *J. Phys. Chem. C,* **114** (2010) 16087.
17. P. Matczak, *Comput. Theor. Chem.,* **1013** (2013) 7.
18. H. Puff and H. Reuter, *J. Organomet. Chem.,* **373** (1989) 173.
19. F. Banse, F. Ribot, P. Toledano, J. Maquet, and C. Sanchez, *Inorg. Chem.,* **34** (1995) 6371.
20. C. Eychenne-Baron, F. Ribot, N. Steunou, C. Sanchez, F. Fayon, M. Biesemans, J. C. Martins, and R. Willem, *Organometallics,* **19** (2000) 1940.
21. Y. Zhang, J. Haitjema, X. Liu, F. Johansson, A. Lindblad, S. Castellanos, N. Ottosson, and A. M. Brouwer, *Proc. SPIE,* **10146** (2017) 1014606.